Effect of Barium on the Properties of Lead Hexaferrite

A. L. Guerrero-Serrano, T.J. Pérez-Juache, M. Mirabal-García, J.A. Matutes-Aquino, S.A. Palomares-Sánchez

Abstract

An analysis of the properties of a family based on lead-barium substitution in the M-type hexaferrite is presented. The samples were prepared by the ceramic method according to the general formula $Pb_xBa_{1-x}Fe_{12}O_{19}$. The barium content was varied with x = 0.1, 0.3, 0.5, 0.7, and 0.9; no secondary phases were detected in any composition. Rietveld refinement analysis was done in order to determinate crystallographic parameters, content of phases and degree of substitution. The effects of the barium on the morphological and magnetic properties were studied. Iron Mössbauer spectroscopy was used for determining the hyperfine parameters of the iron nucleus and their environment; also, the cationic occupancy was evaluated and the results were checked with X-ray refinement results.

Keywords: M-type hexaferrite, Magnetic properties, Rietveld refinement, Cationic substitution, Mössbauer spectroscopy.

Introduction

Hexagonal ferrites form a large family of ferrimagnetic oxides; of these, M-type hexaferrites are the most relevant due to its large variety of applications [1–4]. M-type ferrites are considered the basis of the current ceramic permanent magnet industry [5, 6]. They have a prominent position in the permanent magnet market due to their unique combination of acceptable magnetic performance, low cost and chemical stability [7, 8]. In the 1960s, changes in the properties of binary hexaferrites systems were

investigated, and as a result of these investigations, it was found that there are no sharp kinks on the curves of the properties [9]; this fact suggested that those systems form complete solid solutions between both end members and no special compound can exist at any mixing ratio. It was considered that the improvements on the properties due to substitution might be due to the acceleration of the solid state reaction or sintering process, and not to intrinsic properties of a specific compound [9]. After these investigations, no more further studies were reported. The substitutions have had been given in order to improve specific properties of materials, and in the case of the M-type hexaferrites, it has been determined that the substitution can modify their electrical, magnetic, and crystallography properties [10–12]. The most investigated hexaferrite substitutions in the M-type structure are the barium (M-Ba) and strontium (Sr-M) hexaferrites [13–21]. In the case of lead substituted hexaferrite, only a few works have been reported [22, 23]. A problem with lead compounds is the lead evaporation around 900 °C that produces the formation of secondary phases due an incomplete reaction of the chemical precursors [24].

In this work, pure lead hexaferrite substituted with barium was obtained and the characterization was made in order to determinate what is the influence of the barium substitution on the structural, morphological and magnetic properties; the structural characterization was performed by X-ray diffraction using a GBC Enhanced Mini-Materials Analyzer diffractometer with Cu (Kα) radiation in Bragg–Brentano geometry. The MAUD program has been used for the Rietveld refinement of the structure and to quantify the phases present in the samples [25]; the magnetic characterization was made with a LDJ Electronics VSM9600 vibrating sample magnetometer with H_{max} =

12000 Oe; the Néel temperature has been determined by using a magnetic-TGA technique and the morphology of the samples was observed with a Jeol 1200 electron microscope working at 120 kV. Mössbauer spectrometry was used in order to investigate the effects of the barium substitution on the hyperfine parameters in the nucleus of iron and in their environment at room temperature; a Mössbauer spectrometer was used in regimen of constant acceleration with a source of ^{57}Co in a Rh matrix—each spectrum was fitted with the MossWinn program and the hyperfine parameters were determinated in the function of the degree of barium content.

Experimental Procedure

All the samples were prepared using the ceramic method under the same conditions to avoid effects due to the preparation. The lead oxide (Pb_3O_4); barium carbonate ($BaCO_3$) and iron oxide (α-Fe_2O_3) of analytical grade used as chemical precursors were weighed according to the stoichiometric ratios. The lack of lead was corrected by adding the exact amount of lead oxide that compensates the lost in each sample; the lead excess was calculated from the Rietveld refinement and X-ray data. The powders were mixed in ethylic alcohol for one hour in a rotary mill at 90 rpm.; the mixed powders were dried at 50 °C. Once dried, the powders were subjected to a first heat treatment, called presintering, at 800 °C for one hour. Then the calculated lead excess was added to the powders and mixed during one hour. Two sintering temperatures were tested: 1050 °C and 1100 °C. The sintering time was 2 hours.

The models used in the Rietveld refinement program were constructed on the basis of the lead hexaferrite (hexagonal; space group P 6_3/mmc) [24]. In the Pb^{2+} site, the Ba^{2+}; was added so that the sum of both contributions is always one. The model

used to refined the substituted hexaferrites consist of an close packed arrangement of O^{2-} ions with a barium or lead ion substituting for one O^{2-} in the hexagonal layer. The iron ions are distributed in three octahedral sites (12k, 2a, and $4f_2$), one tetrahedral ($4f_1$), and one bipyramidal (2b). A schematic representation ofM-type structure made by Collomb et al. is available in [26].

Results and discussion

From X-ray characterization, hematite and barium monoferrite was observed a as secondary phase in the samples with a high content of barium and sintered at 1050 °C for x = 0.1(16.7% Wt. α-Fe_2O_3, 3.3% Wt. of $BaFe_2O_4$); and for x = 0.3 (18.9% Wt. α-Fe_2O_3, 6.0% Wt. of $BaFe_2O_4$), which suggests an incomplete reaction of the chemical precursors, due to low temperature of synthesis. In the rest of the samples sintered at 1050 °C, only the M-type phase is present. In the samples sintered at 1100 °C, only the hexaferrite phase is present for all the compositions; see Fig. 1.

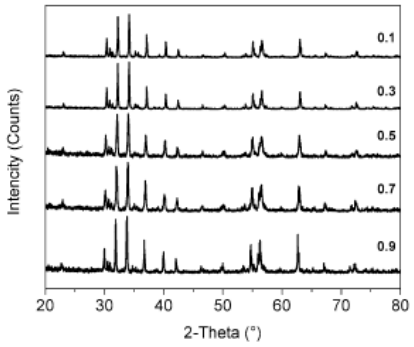

Fig. 1 X-rays diffractograms of $Pb_xBa_{1-x}Fe_{12}O_{19}$ powders sintered at 1100 °C

Table 1 Rietveld refinement of the crystal structure in the M-type substituted hexaferrite

x	Cell parameters		Occupancy (fracc)		Density
	a (Å)	c (Å)	Pb	Ba	Kg/m^3
0.1	5.9020 (1)	23.2075 (10)	0.090 (8)	0.900 (9)	5.29
0.3	5.9017 (2)	23.2019 (11)	0.289 (9)	0.700 (9)	5.35
0.5	5.9019 (1)	23.1970 (9)	0.503 (7)	0.486 (8)	5.43
0.7	5.8992 (1)	23.1557 (9)	0.699 (9)	0.299 (11)	5.51
0.9	5.8979 (1)	23.1502 (10)	0.887 (7)	0.100 (8)	5.56

The crystal structure was refined and the composition of the phases, the structural parameters, and the degree of cationic substitution were obtained. The results are listed in Table 1.

When the barium concentration increases, a slight widening of the unit cell is produced; that is due that the barium ionic radius is larger than the lead ionic radius and this is an indication that the barium is being integrated into the structure. From the refinement of the cationic occupancy, we found that the results are too close to the stoichiometry planned for each sample, which suggests that the loss of lead was compensated adequately and the Ba^{2+} has completely been integrated into the structure of the hexaferrite. As a consequence of the substitution changes in lengths of unit cell are produced (Fig. 2); these changes modify necessarily the superexchange Fe–Fe interactions that are responsible of the ferrimagnetism in the hexaferrite. An important shift on the 12k octahedral site was obtained. A displacement takes place on the plane (*xy*) when the barium content increases. As the Ba^{2+} has a bigger ionic radius when it is incorporated in their corresponding site, it produces a shift along the z axis of the closer layers of O^{2-} (4e and 12k). Figure 3 shows the results in the displacement of the iron 12k site.

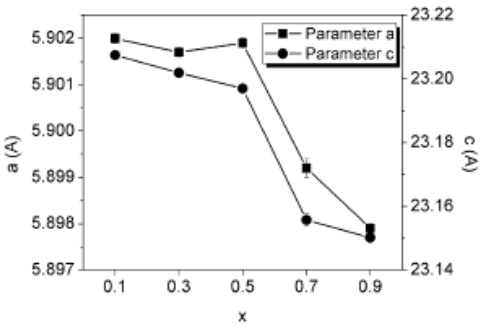

Fig. 2 Cell parameters of $Pb_xBa_{1-x}Fe_{12}O_{19}$ obtained from the Rietveld refinement of the structure

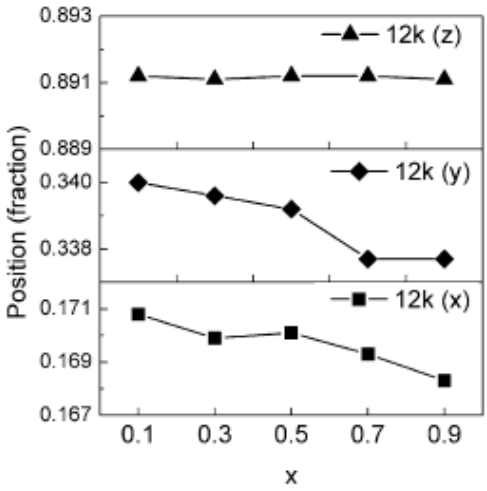

Fig. 3 Shift on the 12k site produced by effect of barium substitution

Mössbauer spectra were obtained for all compositions studied; see Fig. 4. The hyperfine parameters; isomer shift (IS), quadrupole splitting (Q), hyperfine magnetic field (H_{hyp}), and the area of the subspectra were analyzed in terms of the distribution of iron ions over the unit cell by five Zeeman sextets that correspond to five interstitial sites of iron in the structure of the hexaferrite.

The area of each sextet is proportional to site occupancy, and that is possible to estimate the percentage of occupancy in each crystallographic site. Figure 5 shows the occupancy of five interstitial sites of iron. The area of each subspectra was determinated and the sum of areas was normalized to 24. The obtained occupancy of 2b site is lower than their theoretical value; however, the occupancy tends to increase when the barium content decreases; the 2a site presents a slight reduction in their occupancy above x = 0.5; for 4f1, an increase in the occupancy is observed above x = 0.3; and for $4f_2$ the occupancy tends to diminish when the barium content decreases;

the 12k site is approximately maintained in their theoretical value for all compositions. The changes in the occupancy of the sites 2a and 2b are due to vacancy defects [27].

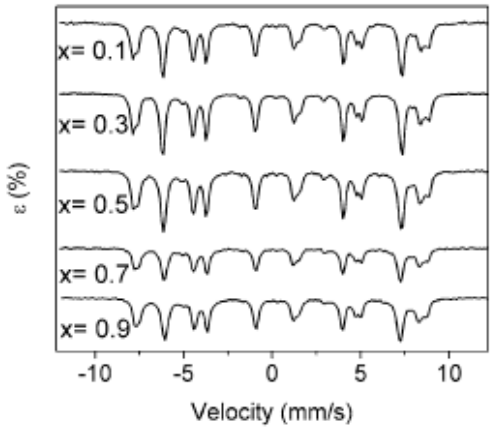

Fig. 4 Mössbauer spectra of lead hexaferrite substituted with different content of barium (x)

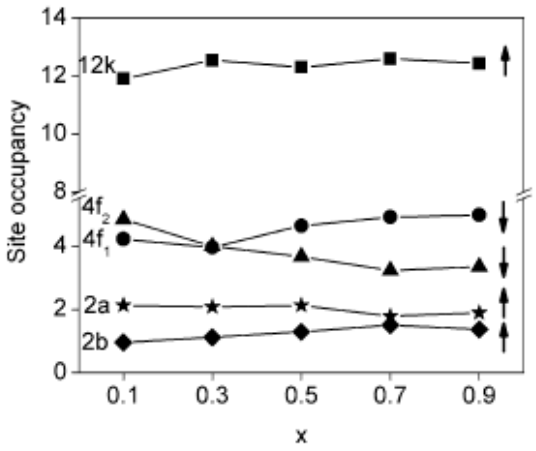

Fig. 5 Fe^{3+} occupancy in function of lead content. The moment of spin of iron is represent by the *arrow* in each site

The values obtained for the isomer shift in the substituted samples are related with the iron with valence 3+; typical values are between 0.3 and 0.7 mm/s, while for the iron with valence 2+, are between 1.1 and 1.3 mm/s [28]. Figure 6 shows the results of the isomer shift; for 12k, it is approximately constant, while for 4f2 and 4f1 a slight increase is observed for x = 0.5; for 2a and 2b there is a reduction on x = 0.5. These

variations are produced by the effect of the barium substitution affecting the electron density in the vicinity of the iron sites, principally on the 2a, 2b, and 4f1. A reduction on isomer shift values is attributed with an increase of the electron density in the vicinity of these sites [29]. Figure 7 shows the quadrupolar shift in function of the barium content; the quadrupolar shift is related with the symmetry around each one of the iron sites. Deviation of the symmetry in the closer environment produces an increase in their corresponding quadrupolar shift. From data reported in Fig. 7, a strong increase in the quadrupolar shift of the 2b site is observed when barium content increases; also, slight variations are observed for 2a, 4f1, and 4f2 sites when $x = 0.5$.

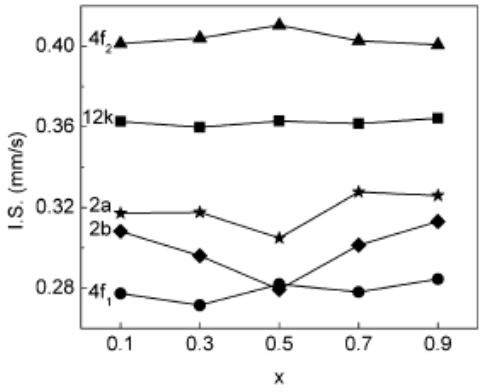

Fig. 6 Isomer shift (*IS*) of the Fe^{3+} contributions for different sites

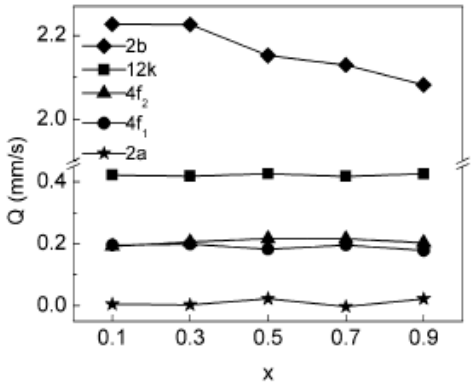

Fig. 7 Quadrupolar shift (*Q*) of the Fe^{3+} contributions for different sites

The quadrupolar shift of the 12k site is approximately maintained without changes. In the 2b site, the change in quadrupolar shift is related with an increment in occupancy of this site that generates an increase of the crystallographic symmetry. When the barium content increases, the bipyramid formed by O^{2-} tends to be more asymmetric [30]; for x = 0.5, we can deduce a slight readjustment of the electron density around the iron sites takes place that is produced by an increase of the barium content in the structure of the hexaferrite.

Figure 8 shows a decrease in the hyperfine magnetic field value in all sites when the barium content decreases. This reduction is gradual and is proportional to the nuclear magnetic moment. The results are in agreement with the expected due to the lower magnetization of the lead hexaferrite [31–33].

The magnetic characterization was made in order to determine the effect of the barium substitution on the magnetic properties of the hexaferrite. Figure 9 shows the hysteresis loops obtained at room temperature. It is possible to observe changes in the hysteresis loops when the barium content increases. Table 2 shows the values for the magnetic parameters' measurements. The Néel temperature (TN) also was obtained from the magnetic-TGA technique and the samples present a lower Néel temperature than the pure Barium hexaferrite (~450 °C). Although for x = 0.5, a considerable increase on the T_N can be observed. This increase may be related with the changes in the isomer shift observed for this composition.

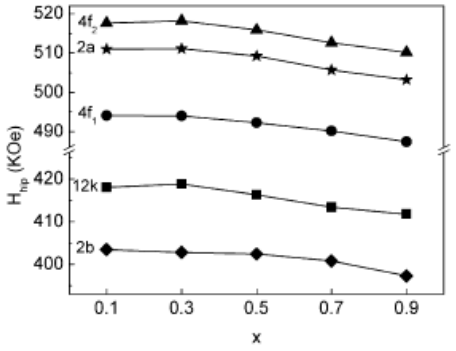

Fig. 8 Hyperfine magnetic field (H_{hyp}) contributions for the crystallographic sites of the Fe^{3+}

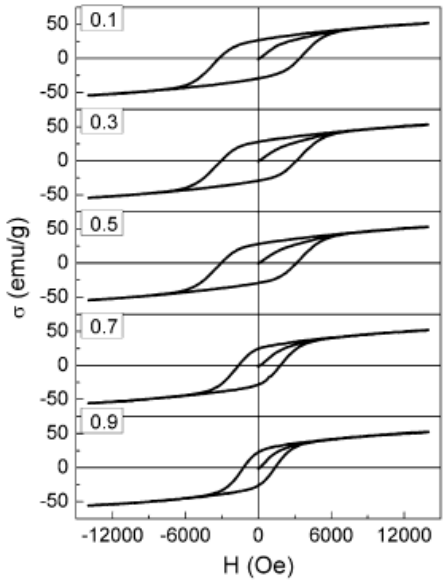

Fig. 9 Hysteresis loops of the $Pb_xBa_{1-x}Fe_{12}O_{19}$, sintered at 1100 °C

Micrographs obtained from SEM are present in Fig. 10; we can observe the effect of the barium substitution on the grain size and in the morphology of the particles. From samples with low barium content (x = 0.9), typical sizes and morphologies of hexagonal plates between 1.0 and 2.0 μmof diameter were found. When the content of barium increases, the particle size decreases and for x = 0.1 the average diameter is around 0.5 μm.

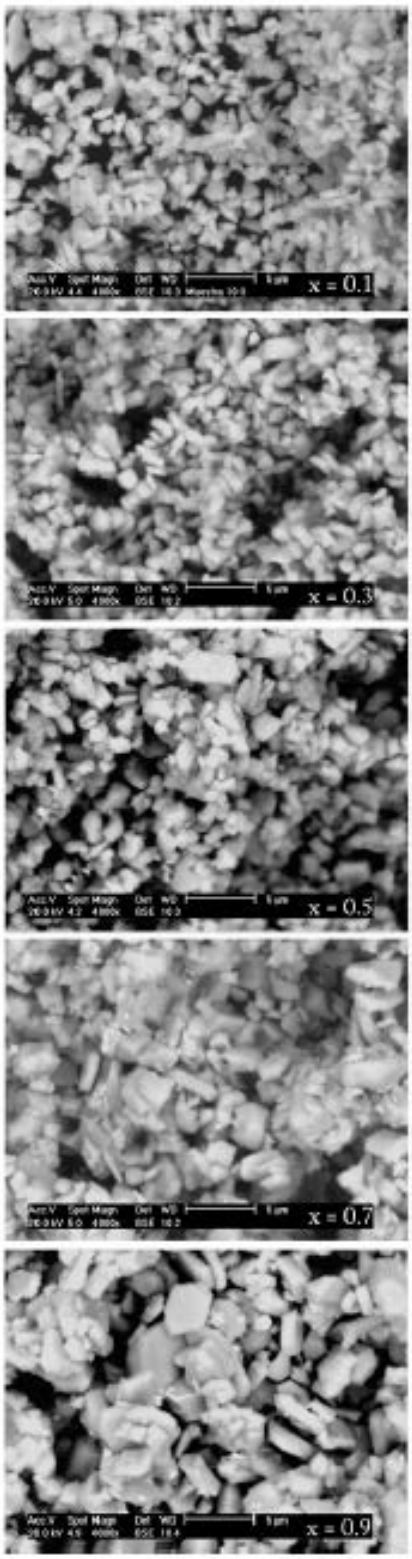

Fig. 10 SEM image of $Pb_xBa_{1-x}Fe_{12}O_{19}$ powders

Table 2 Effect of the barium substitution on the magnetic properties

	0.1	0.3	0.5	0.7	0.9
σ_s (emu/g)	52.07	54.52	51.51	53	52.8
σ_r (emu/g)	26.9	28.1	25.3	24.57	22.77
H_c (Oe)	3299	3091	2523	1689	1289
T_N (°C)	435	428	445	426	425

Conclusion

Polycrystalline substituted hexaferrite ($Pb_xBa_{1-x}Fe_{12}O_{19}$) were successfully prepared by the ceramic method. The accurate determination of the loss of lead by means of Rietveld refinement allows to obtain the hexaferrite without secondary phases. The best temperature to form the phase was 1100 °C, which means 150 °C below the temperature required to form the barium hexaferrite.

According to the results, we have that the substitution with barium in the lead hexaferrite simultaneously modified the crystal structure, the particle size and morphology, and the magnetic properties. These changes are gradual and depend of the barium content.

Mössbauer spectroscopy and X-ray diffraction are two techniques which complement successfully in the accurate study of the crystallographic structure; The barium, when entering on the structure, produces changes in the oxygen layers due to the large ionic size of barium; a displacement of oxygen layers which produces a shift on the iron 12k site was detected, without changes in symmetry. For the iron 2b site, defects of vacancy were detected; the vacancies tend to diminish when the barium

content increases. The magnetic parameters and the hyperfine field show a clear trend to increase gradually when the barium content is increased.

References

1. Leccabue, F., Panizzieri, R., Garcia, S., Suarez, N., Sánchez, J.L., Ares, O., Hua, X.R.: J. Mater. Sci. 25, 2765 (1990)

2. Matsuoka,M., Naoe,M., Okayama, O., Ku, M., Hoshi, Y.: J. Appl. Phys. 57, 4040 (1985)

3. Machida, H., Ohmi, F., Sawada, Y., Kaneko, Y.,Watada, A., Nakamura, H.: J. Magn. Magn. Mater. 54–57, 1399 (1986)

4. Sugimoto, M.: J. Am. Ceram. Soc. 82, 269 (1999)

5. Harris, V.G., Chen, Z., Chen, Y., Yoon, S., Sakai, T., Gieler, A., Yang, A., He, Y., Ziemer, K.S., Sun, N.X., Vittoria, C.: J. Appl. Phys. 99, 08M911 (2006)

6. Valenzuela, R.: Magnetic Ceramics. Cambridge University Press, New York (1994)

7. Zi, Z.F., Sun, Y.P., Zhu, X.B., Yang, Z.R., Dai, J.M., Song, W.H.: J. Magn. Magn. Mater. 320, 2746 (2008)

8. Kools, F., Morel, A., Grössinger, R., Le Breton, J.M., Tenaud, P.: J. Magn. Magn. Mater. 242, 1270 (2002)

9. Kojima, H.: Ferromagnetic Materials, vol. 3. North-Holland, Amsterdam (1982)

10. Wang, L., Qiang, H., Lei, M., Qitu, Z.: J. Rare Earths 25, 216 (2007)

11. Tenaud, P., Morel, A., Kools, F., Breton, J.M.L., Lechevallier, L.: J. Alloys Compd. 370, 331 (2004)

12. Litsardakis, G., Manolakis, I., Serletis, C., Efthimiadis, K.G.: J. Magn. Magn. Mater. 316, 170 (2007)

13. Javed, M., Naeem, M., Hernandez-Gomez, P., Maria, J.M.: J. Magn. Magn. Mater. 320, 881 (2008)

14. Litsardakis, G., Manolakis, I., Serletis, C., Efhimiadis, K.G.: J. Appl. Phys. 103, 07E501 (2008)

15. Winotai, P., Thongmee, S., Tang, I.M.: Mater. Res. Bull. 35, 1747 (2000)

16. Pereira, F.M.M., Junior, C.A.R., Santos, M.R.P., Sohn, R.S.T.M., Freire, F.N.A., Sasaki, M., de Paiva, J.A.C., Sombra, A.S.B.: J. Mater. Sci. 19, 627 (2008)

17. Lixi, W., Qiang, H., Lei, M., Qitu, Z.: J. Rare Earths 25, 216 (2007)

18. Litsardakis, G., Manolakis, I., Serletis, C., Efhimiadis, K.G.: J. Magn. Magn. Mater. 316, 170 (2007)

19. Liu, X., Hernández-Gómez, P., Huang, K., Zhou, S., Wang, Y., Cai, X., Sun, H., Ma, B.: J. Magn. Magn. Mater. 305, 524 (2006)

20. Liu, X., Zhong, W., Yang, S., Yu, Z., Gu, B., Du, Y.: J. Magn. Magn. Mater. 238, 207 (2002)

21. Sharma, P., Verma, A., Sidhu, R.K., Pandey, O.P.: J. Alloys Compd. 361, 257 (2003)

22. Albanese, G., Watts, B.E., Leccabue, F., Diaz-Castañon, S.: J. Magn. Magn. Mater. 184, 337 (1998)

23. Albanese, G., Díaz-Castañón, S., Leccabue, F., Watts, B.E.: J. Mater. Sci. 35, 4415 (2000)

24. Palomares-Sánchez, S.A., Díaz-Castañon, S., Ponce-Castañeda, S., Mirabal-García, M., Leccabue, F., Watts, B.E.: Mater. Lett. 59, 591 (2005)

25. Ferrari, M., Lutterotti, L.: J. Appl. Phys. 76, 7246 (1994)

26. Collomb, A., Lambert Andron, B., Boucherle, J.X., Samaras, D.: Phys. Status Solidi A 96, 385 (1986)

27. Herme, C., Jacobo, S.E., Bercoff, P.G., Arcondo, B.: Hyperfine Interact. 195, 205 (2010)

28. Drago, R.S.: Physical Methods in Inorganic Chemistry. Rheinhold, New York (1965)

29. Lechevillier, L., Le Breton, J.M., Teillet, J., Morel, A., Kools, F., Tenaud, P.: Physica B 327, 135 (2003)

30. Sauer, Ch., Köbler, U., Zinn, W., Stäblen, H.: J. Phys. Chem. Solids 39, 1197 (1978)

31. Martirosyan, K.S., Martirosyan, N.S., Chalykh, A.E.: Inorg. Mater. 39, 866 (2003)

32. Díaz-Castañon, S., Faloh-Gandarilla, J.C., Leccabue, F., Albanese, G.: J. Magn. Magn. Mater. 272–276, 2221 (2004)

33. Yang, N., Yang, H., Jia, J., Pang, X.: J. Alloys Compd. 438, 263

(2007)